arXiv:2002.11433v1 [cs.CV] 26 Feb 2020

Efficient Semantic Video Segmentation with Per-frame Inference*

Yifan Liu[1], Chunhua Shen[1], Changqian Yu[2,1], Jingdong Wang[3]

[1] The University of Adelaide, Australia
[2] Huazhong University of Science and Technology, China
[3] Microsoft Research

Abstract. In semantic segmentation, most existing real-time deep models trained with each frame independently may produce inconsistent results for a video sequence. Advanced methods take into considerations the correlations in the video sequence, e.g., by propagating the results to the neighboring frames using optical flow, or extracting the frame representations with other frames, which may lead to inaccurate results or unbalanced latency. In this work, we process efficient semantic video segmentation in a per-frame fashion during the inference process.
Different from previous per-frame models, we explicitly consider the temporal consistency among frames as extra constraints during the training process and embed the temporal consistency into the segmentation network. Therefore, in the inference process, we can process each frame independently with no latency, and improve the temporal consistency with no extra computational cost and post-processing. We employ compact models for real-time execution. To narrow the performance gap between compact models and large models, new knowledge distillation methods are designed. Our results outperform previous keyframe based methods with a better trade-off between the accuracy and the inference speed on popular benchmarks, including the Cityscapes and Camvid. The temporal consistency is also improved compared with corresponding baselines which are trained with each frame independently.
Code is available at: https://tinyurl.com/segment-video

Keywords: semantic video segmentation, real-time, temporal consistency

1 Introduction

Semantic segmentation, a fundamental task in computer vision, aims to assign a semantic label to each pixel in an image. In recent years, the development of deep learning has brought significant success to the task of image semantic segmentation [40, 34, 4] on benchmark datasets, but often with a high computational cost. This task will be even more expensive when extending to the video

* CY's contribution was made when visiting The University of Adelaide. CS is corresponding author: chunhua.shen@adelaide.edu.au

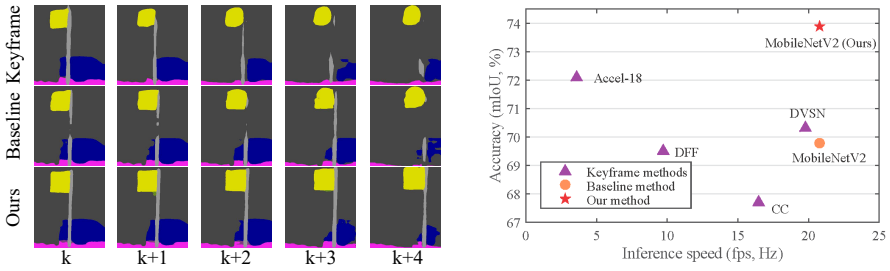

(a) Visualization results (b) Accuracy vs. inference speed.

Fig. 1 – **(a)** Keyframe: Accel [14] propagates and fuses the results from the keyframe (k) to others ($k+1, \dots$), which results poor results on other frames. Baseline method: training the model on single frames and inferring the segmentation on single frames separately will produce temporal inconsistent results. Our method: training the model with the correlations among frames and inferring the segmentation on single frames separately will produce high quality and smooth results. **(b)** Comparing our enhanced MobileNetV2 model with previous keyframe based methods: Accel [14], DVSN [36], DFF [42] and CC [30]. The inference speed is evaluated on a single GTX 1080Ti.

domain. Due to the demand for real-world applications, e.g., autonomous driving and robotics, it is challenging but crucial to build a fast and accurate video semantic segmentation system.

Previous works for semantic video segmentation can be categorized into two types. The first group focuses on improving the performance for video segmentation by adding post-processing among frames [20], or employing extra modules to use multi-frames information during inference [9]. The high computational cost makes it hard to apply to mobile devices. The second group employs a keyframe policy to handle some important frames with more computation cost, then copy [30] or propagate [42, 41, 36] the outputs or the feature maps to other frames in between by optical flows. The keyframe based methods can work well in acceleration for the average cost. However, it requires different inference time for keyframes and other frames, which results in an unbalanced latency. Besides, the performance will worsen on frames far away from the keyframe due to the cumulative warping error, for example, the first row in Figure 1(a).

Clearly, the latency will be alleviated by processing each frame independently during inference while the real-time execution can be enabled by choosing compact networks [1, 27, 22]. However, previous works [25, 40] directly training the model on each frame independently will produce temporal inconsistent results on the video sequence as shown in the second row of Figure 1(a). To address the above problems, we explicitly consider the temporal consistency among frames as extra constraints during the training process and employ compact networks with per-frame inference manners to ease the problem of latency and achieve the real-time speed.

A motion guided *temporal loss* is employed with the motivation of assigning a consistent label to the same pixel along the time step. A motion estimation

network is introduced to predict the motion (e.g., optical-flow) of each pixel from the current frame to the next frame based on the input frame-pair. Predicted semantic labels are propagated to the next frame to supervise predictions of the next frame. Therefore, the temporal consistency is encoded into the segmentation network through this constraint.

To narrow the performance gap between compact models and large models, we design new *temporal consistency knowledge distillation* items to help the training of compact models. Distillation methods are widely used in image recognition tasks [21, 12, 18], and achieve great success. Different from previous distillation methods, which only consider the spatial correlations, we embed the temporal consistency into distillation items. We extract the pair-wise frames dependency by calculating the pair-wise similarities for different locations between two frames, and further encode the multi-frames dependency into a latent embedding by using a recurrent unit, ConvLSTM [31]. The new distillation methods not only improve temporal consistency but also boost segmentation accuracy. We also include the spatial knowledge distillation methods [21] of single frames in training to further improve the accuracy.

We evaluate the proposed methods on widely-used semantic video segmentation benchmarks: Cityscapes [7] and Camvid [2]. Different compact networks, i.e., PSPNet18 [40], MobileNetV2 [29] and a light weight HRNet [33], are included to verify that the proposed methods can empirically improve the segmentation accuracy and the temporal consistency, without any extra computation and post-processing during inference. The proposed methods also show superiority in the trade-off of accuracy and the inference speed, for example, with the per-frame inference fashion, our enhanced MobileNetV2 [29] can achieve higher accuracy with a faster inference speed compared with state-of-the-art keyframe based methods as shown in Figure 1(b). We summarize our main contributions as follows.

- We process semantic video segmentation with compact models by per-frame inference, with no post-processing and extra computational cost, enabling a real-time inference speed without latency. We design new knowledge distillation methods to signicantly improve the training.
- We explicitly consider the temporal consistency in the training process by using a temporal loss and newly designed temporal consistency knowledge distillation methods.
- Empirical experiment results on Cityscapes and Camvid show that with the help of proposed training methods, the compact models outperform previous state-of-the-art semantic video segmentation methods with a better trade-off between accuracy and inference speed.

1.1 Related Work

Semantic Video Segmentation. Semantic video segmentation requires dense labeling for all pixels in each frame of a video sequence. It is different from video object detection [35] and video object segmentation [6], which only focus on the

recognition of foreground objects. Previous work can be summarized into two streams.

The first one focuses on improving the accuracy by exploiting the temporal relations and the unlabelled data in the video sequence. Nilsson and Sminchiesescu [24] employ a gated recurrent unit to propagate semantic labels to unlabeled frames. Other works like NetWarp [9], STFCN [8], and SVP [20] also employ optical-flow or recurrent units to fuse the results of several frames during inferring to improve the segmentation accuracy. Recently, Zhu *et al.* [43] propose to use a motion estimation network to propagate ground truth labels to unlabeled frames as data augmentation and achieve state-of-the-art performance with the segmentation accuracy. These methods can achieve significant performance, but are hard to apply to mobile devices

Another stream pays attention to reduce the computational cost by re-using the feature maps in the neighboring frames. ClockNet [30] proposes to copy the feature map to the next frame directly, therefore, can reduce the computational cost. DFF [42] employs the optical flow to warp the feature map between the keyframe and other frames. Xu *et al.* [36] further propose to use an adaptive keyframe selection policy while Zhu *et al.* [41] find out that propagating partial region in the feature map can get better performance. Li *et al.* [19] propose a low-latency video segmentation network by optimizing both the keyframe selection and the adaptive feature propagation. Accel [14] proposes a network fusion policy to use a large model to predict the keyframe and use a compact one in other frames. They also employ optical flow to propagate results of the keyframe for results fusion. Keyframe based methods require different inference time and may produce different quantity results between keyframes and other frames. Besides, the keyframe based methods need to refer to previous prediction results during the inference process, which may cause unbalanced latency. In this work, we solve the real-time video segmentation by per-frame inference with the compact network, and propose a temporal loss and the temporal consistency knowledge distillation to ensure both better performance and temporal consistency.

Temporal Consistency. Applying image processing algorithms to each frame of a video may lead to inconsistent results. The temporal consistency problem has draw much attention in low-level applications, such as task-specific methods including colorization [17], in-painting [15] and style transfer [10] and task blind approaches [16, 37]. The temporal consistency is also essential in semantic video segmentation. Miksik *et al.*. [23] employ a post-processing method that learns a similarity function between pixels of consecutive frames to propagate predictions across time. Nilsson and Sminchiesescu [24] insert the optical flow estimation network into the forward pass and employ a recurrent unit to make use of neighbouring predictions. Our method is more efficient than them because we employ a per-frame inference fashion. The warped previous predictions work as a constraint (not extra input information) during training. Therefore, we do not need to depend on other frames during inferring, which reduces the latency and enables the probability of processing all the frames in parallel.

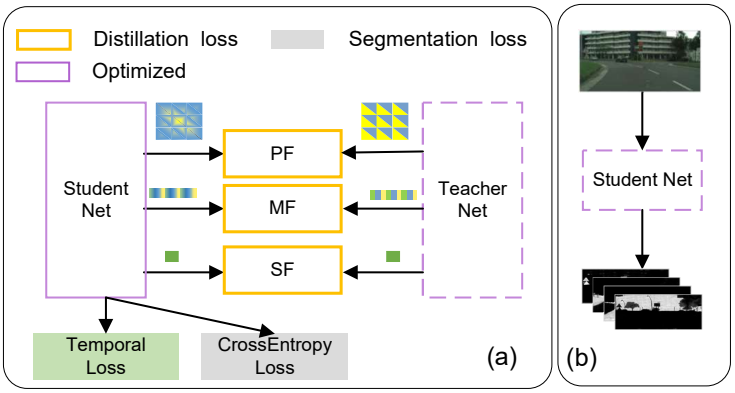

Fig. 2 – (a) **Overall of proposed training schemes**: We apply the distillation loss and the temporal loss to improve the accuracy as well as the smoothness. PF (pair-wise-frame dependency) and MF (Multi-frame dependency) represent the temporal consistency knowledge distillation method we proposed. SF (Single-frame dependency) represents the knowledge distillation method on the single image proposed by Liu et al. [21]. (b) **The inference process**. All the proposed methods are only applied during training. We do not introduce any parameters or post-processing during inferring.

Knowledge Distillation. The effectiveness of knowledge distillation has been verified in classification [13, 28, 38]. The output of the large teacher net, including the final logits and the intermediate feature maps, are treated as soft targets to supervise the compact student net. The follow-up works have applied knowledge distillation to various applications with modification, such as distilling feature maps in interest object regions in object detection [18], distilling the ranking correlations among samples for person re-identification task [5], and distilling the structure information in semantic segmentation [12, 21]. Previous knowledge distillation methods in semantic segmentation [12, 21] design distillation items only for improving the segmentation accuracy and can not improve the temporal consistency. In this work, we focus on encoding the motion information into the distillation items to make the segmentation networks more suitable for the semantic video segmentation tasks.

2 Approach

In Figure 2, we show the overall of our proposed methods, including **a temporal loss**, which enhances the temporal consistency for segmentation network, and the **temporal consistency knowledge distillation**, i.e., pair-wise-frame (PF) dependency and multi-frame (MF) dependency. The single-frame (SF) distillation [21] is also employed to further improving the segmentation accuracy, and details can be found in Section S1.1 in supplementary materials.

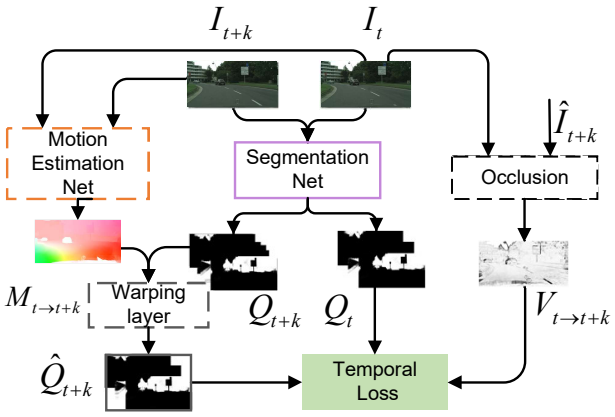

Fig. 3 – **Temporal loss** is applied to the training of segmentation networks, including the teacher net and the student net. We use the warped prediction of previous frames to supervise the prediction of the current frame.

2.1 Motion Guided Temporal Consistency

Training semantic segmentation networks independently on each frame of a video often leads to undesired inconsistency. Conventional methods consider adding previous predictions as an extra input, which introduce extra computational cost during inferring. We employ previous predictions as supervised signals to assign consistent labels to each corresponding pixel following the time steps.

As shown in Figure 3, for two input frames $\mathbf{I}_t$, $\mathbf{I}_{t+k}$ from time t and $t+k$, we have:

$$\ell_{tl}(\mathbf{I}_t, \mathbf{I}_{t+k}) = \frac{1}{N}\sum_{i=1}^{N} V_{t\Rightarrow t+k}^{(i)} \left\|\mathbf{q}_t^i - \hat{\mathbf{q}}_{t+k\Rightarrow t}^i\right\|_2^2 \tag{1}$$

where $\mathbf{q}_t^i$ represents the predicted class probability at the position i of the segmentation map $\mathbf{Q_t}$, and $\hat{\mathbf{q}}_{t+k\Rightarrow t}^i$ is the warped class probability from frame $t+k$ to frame t, by using a motion estimation network $f(\cdot)$. Such an $f(\cdot)$ can predict the amount of motion changes in the x and y directions for each pixel: $f(\mathbf{I}_{t+k}, \mathbf{I}_t) = \mathbf{M}_{t\to t+k}$, where $\delta i = \mathbf{M}_{t\to t+k}(i)$, indicating the pixel on the position i of the frame t moves to the position $i+\delta i$ in the frame $t+k$. Therefore, the the segmentation maps between two input frames are aligned by the motion guidance. An occlusion mask $\mathbf{V}_{t\Rightarrow t+k}$ is designed to remove the noise caused by the warping error: $\mathbf{V}_{t\Rightarrow t+k} = \exp(-\left|\mathbf{I}_t - \hat{\mathbf{I}}_{t+k}\right|)$, where $\hat{\mathbf{I}}_{t+k}$ is the warped input frame. We employ a pre-trained optical flow prediction network as the motion estimation net in implementation. We directly consider the temporal consistency during the training process through the motion guided temporal loss by constraining a moving pixel along the time steps to have a consistent semantic label.

2.2 Temporal Consistency Knowledge Distillation

To train the compact networks effectively, we build a distillation mechanism to train the compact student net S by making use of cumbersome teacher net T. The teacher net T is already well-trained with the cross-entropy loss and the temporal loss to achieve a high temporal consistency as well as the segmentation accuracy. Two new distillation items are designed to transfer the temporal consistency from T to S. We also employ the pixel-wise distillation, and the pair-wise distillation proposed in [21] on every single frame to improve the segmentation accuracy, named 'SF' in Figure 2.

Pair-wise-Frames Dependency. We introduce an attention (AT) operator to calculate the pair-wise similarity map $\mathbf{A}_{\mathbf{X}_1,\mathbf{X}_2}$ of two input tensors $\mathbf{X}_1, \mathbf{X}_2$, where $\mathbf{A}_{\mathbf{X}_1,\mathbf{X}_2} \in \mathbb{R}^{N\times N\times 1}$ and $\mathbf{X}_1, \mathbf{X}_2 \in \mathbb{R}^{N\times C}$. For the pixel a_{ij} in $\mathbf{A}$, we calculate the cosine similarity between $\mathbf{x}_1^i$ and $\mathbf{x}_2^j$ from $\mathbf{X}_1$ and $\mathbf{X}_2$, respectively: $a_{ij} = {\mathbf{x}_1^i}^\top \mathbf{x}_2^j / (\|\mathbf{x}_1^i\|_2 \|\mathbf{x}_2^j\|_2)$. It is an efficient and easy way to encode the correlations between two input tensors.

As shown in Figure 4-(a), we encode the pair-wise dependency between the prediction of every two neighboring frame pairs by using the AT operator, and get the similarity map $\mathbf{A}_{\mathbf{Q}_t,\mathbf{Q}_{t+k}}$, where $\mathbf{Q}_t$ is the segmentation map of frame t and a_{ij} of $\mathbf{A}_{\mathbf{Q}_t,\mathbf{Q}_{t+k}}$ denotes the similarity between the class probabilities on the location i of the frame t and the location j of the frame $t+k$. If a pixel on the location i of frame t moves to location j of frame $t+k$, the similarity a_{ij} may be higher. Therefore, the pair-wise dependency can reflect the motion correlation between two frames.

We align the pair-wise-frame (PF) dependency between the teacher net T and the student net S,

$$\ell_{PF}(\mathbf{Q_t}, \mathbf{Q_{t+k}}) = \frac{1}{N^2} \sum_{i=1}^{N} \sum_{j=1}^{N} (a_{ij}^{\mathsf{S}} - a_{ij}^{\mathsf{T}})^2, \tag{2}$$

where $\forall a_{ij}^{\mathsf{S}} \in \mathbf{A}_{\mathbf{Q}_t,\mathbf{Q}_{t+k}}^{\mathsf{S}}$ and $\forall a_{ij}^{\mathsf{T}} \in \mathbf{A}_{\mathbf{Q}_t,\mathbf{Q}_{t+k}}^{\mathsf{T}}$.

Multi-Frame Dependency. As shown in Figure 4-(b), for a video sequence $\mathcal{I} = \{\dots \mathbf{I}_{t-1}, \mathbf{I}_t, \mathbf{I}_{t+1} \dots\}$, we extract corresponding feature maps $\mathcal{F} = \{\dots \mathbf{F}_{t-1}, \mathbf{F}_t, \mathbf{F}_{t+1} \dots\}$ from the output of the last convolutional block before the classification layer, and then calculate a self-similarity map, $\mathbf{A}_{\mathbf{F}_t,\mathbf{F}_t}$, for each frame by using AT operator in order to: 1) capture the structure information among pixels, and 2) align the different feature channels between the teacher net and student net.

We employ a ConvLSTM unit to encode the sequence of self-similarity maps into an embedding $\mathbf{E} \in \mathbb{R}^{1\times D_e}$, where D_e is the length of the embedding space. For each time step, the ConvLSTM unit takes $\mathbf{A}_{\mathbf{F}_t,\mathbf{F}_t}$ and the hidden state which contains the information of previous $t-1$ frames as input and gives an output embedding $\mathbf{E}_t$ along with the hidden state of the current time step. We align the final output embedding [4] at the last time step, $\mathbf{E}^{\mathsf{T}}$ and $\mathbf{E}^{\mathsf{S}}$ from T and S,

[4] The details of calculations in ConvLSTM is referred in [31], and we also include the key equations in Section S1.2 in supplementary materials.

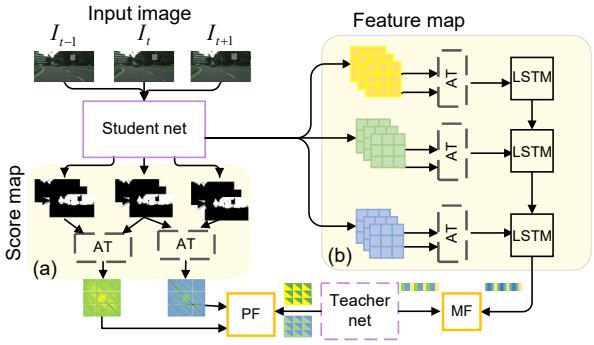

Fig. 4 – (a) **pair-wise-frame dependency (PF)**: encode the motion relations between two frames. (b) **multi-frame dependency (MF)**: extract the correlations of the intermediate feature maps among multi-frame. AT is the attention operator which calculates the pair-wise similarity of each spatial location.

respectively. The output embedding encodes the relations of the whole input sequence, named multi-frame dependency (MF). The distillation loss based on multi-frame dependency is termed as: $\ell_{MF}(\mathcal{F}) = \left\|\mathbf{E}^{\mathsf{T}} - \mathbf{E}^{\mathsf{S}}\right\|_2^2$.

The parameters in the ConvLSTM unit are optimized together with the student net. To extract the multi-frame dependency, both the teacher net and the student net share the weight of the ConvLSTM unit. Note that there exists a model collapse point when the weights and bias in the ConvLSTM are all equal to zero. We clip the weights of ConvLSTM between a certain range and enlarges the $\mathbf{E}^{\mathsf{T}}$ as a regularization to prevent the model collapse.

2.3 Optimization

As illustrated in Figure 2, we pre-train the teacher net with the segmentation loss and the temporal loss to get a segmentation network with the high semantic accuracy and temporal consistency. When optimizing the student net, we fix the weight of the teacher net and the motion estimation net. These two parts are only used to calculate the temporal loss and the distillation items, which can be seen as extra regularization items during the training of the student net. The whole objective function for a sampled video sequence consists of the conventional cross-entropy loss ℓ_{ce}, the single-frame distillation loss ℓ_{SF}, temporal loss, and the temporal consistency distillation items:

$$\ell = \sum_{t=1}^{T'} \ell_{ce}^{(t)} + \lambda\Big(\sum_{t=1}^{T} \ell_{SF}^{(t)} + \sum_{i=1}^{T-1} \ell_{tl}(\mathbf{Q}_t, \mathbf{Q}_{t+1}) + \sum_{i=1}^{T-1} \ell_{PF}(\mathbf{Q}_t, \mathbf{Q}_{t+1}) + \ell_{MF}\Big), \tag{3}$$

where T is the number of all the frames in one training sequence, and T' is the number of labeled frames. Due to the high labeling cost in semantic video

segmentation tasks [7, 2], most of the datasets are only annotated with sparse frames. Our methods can be easily applied to the sparse-labeled dataset, because 1) we can make use of large teacher models to generate soft targets; and 2) we care about the temporal consistency between two frames, which can be self-supervised through motion. The loss weight for all regularization items λ is set to 0.1.

After training the compact network, all the motion-estimation net, teacher net, and the distillation modules can be removed. We only keep the student net as the semantic video segmentation network. Thus, both the segmentation accuracy and the temporal consistency can be improved with no extra computational cost in the per-frame inference process.

3 Implementation details

Dataset. We evaluate our proposed method on Camvid [2] and Cityscapes [7], which are standard benchmarks for semantic segmentation [14, 30, 24]. Cityscapes [7] is collected for urban scene understanding and contains 30-frame snippets of the street scene with 17 frames per second The dataset contains $5,000$ high quality pixel-level finely annotated images at 20^{th} frame in each snippets, which are divided into $2,975$, 500, $1,525$ images for training, validation and testing. The CamVid dataset [2] is an automotive dataset. It contains five different videos, which has ground truth labels every 30 frames. Three train videos contain 367 frames, while two test videos contain 233 frames.

Network structures. Different from keyframe based method, which takes several frames as input during inferring, we employ a compact segmentation model with per-frame inference. There are three main parts while training the system:

- A light-weight segmentation network. We conduct most of the experiments on ResNet18 with the architecture of PSPnet [40], namely PSPNet18. We also employ MobileNetV2 [29] and a light-weight HRNet-w18 [33] to verify the effectiveness.
- A motion estimation network. We use a pretrained FlowNetV2 [26] to predict the motion between two frames. Because this module can be removed during inferring, we do not need to consider employing a lightweight flownet for acceleration, like in DFF [42] and GRFP [24].
- A teacher network. We adopt widely-used segmentation architecture PSPNet [40] with a ResNet101 [11] as the teacher network, namely PSPNet101, which is used to calculate the soft targets in distillation items. We train the teacher net with the temporal loss to enhance the temporal consistency of the teacher.

Random sampled policy. In order to reduce the computational cost while training video data, and make use of more unlabeled frames, we randomly sample frames in front of the labeled frame, named 'frame_f' and behind of the labeled frame, named 'frame_b' to form a training triplet (frame_f, labeled frame, frame_b), instead of only using the frames right next to the labeled ones. The

Table 1 – Accuracy and temporal consistency on Cityscapes validation set. SF: single-frame distillation methods, PF: our proposed pair-wise-frame dependency distillation method. MF: our proposed multi-frame dependency distillation method, TL: the temporal loss. The proposed distillation methods and temporal loss can improve both the temporal consistency and accuracy, and they are complementary to each other.

Scheme index	SF	PF	MF	TL	mIoU	Pixel accuracy	Temporal consistency
a					69.79	77.18	68.50
b	✓				70.85	78.41	69.20
c		✓			70.32	77.96	70.10
d			✓		70.38	77.99	69.78
e				✓	70.67	78.46	70.46
f		✓	✓		71.16	78.69	70.21
g	✓	✓	✓		72.01	79.21	69.99
h	✓	✓	✓	✓	**73.06**	**80.75**	**70.56**

random sampled policy can take both long term and short term correlations into consideration, and achieve better performance. Training on a longer sequence may have better performance, however, it is not friendly to the hardware resource.

Training and inference. On Cityscapes, the segmentation networks in this paper are trained by mini-batch stochastic gradient descent (SGD) for 200 epochs. We sample 8 training triplets for each mini-batch. The learning rate is initialized as 0.01 and is multiplied by $(1 - \frac{iter}{max-iter})^{0.9}$. We random cut the images into 769×769 as the training input. Normal data augmentation methods are applied during training, such as random scaling (from 0.5 to 2.1) and random flipping. On Camvid, we use a crop size of 640×640. We use the official implementation of PSPNet in Pytorch[39] and train all the network with 4 cards of Tesla Volta 100.

Evaluation Metrics. We evaluate our method with three aspects: accuracy, temporal consistency, and efficiency. The accuracy is evaluated by popular used mean Intersection over Union (mIoU) and pixel accuracy for semantic segmentation [21]. We report the model parameters (#Param) and frames per second (fps) to show the efficiency of employed networks. We follow [16] to measure the temporal stability of a video based on the flow warping error between two frames. Different from [16], we use the mIoU score instead of the mean square error to evaluate the semantic segmentation results, and more details can be found in Section 2.1 of Appendix. We also attach video results to show the improvement of the temporal stability.

4 Experiments

4.1 Ablations

All the ablation experiments are conducted on the Cityscapes dataset with the PSPNet18. The temporal consistency is evaluated with the whole image in a single scale.

Effectiveness of proposed methods. In this section, we verify the effectiveness of the proposed training scheme. Both the accuracy and temporal consistency are shown in 1. We build the baseline scheme a, which is trained on every labeled single frame. Then, we apply three distillation items: the single-frame dependency (SF), the pair-wise-frame dependency (PF) and multi-frame dependency (MF), separately, to get the scheme b, c and d. The temporal loss is employed in the scheme e. Compared with the baseline scheme, all the schemes can improve accuracy as well as temporal consistency. To compare scheme b with c and d, one can see that the distillation scheme across frames can improve the temporal consistency to a greater extent. From the scheme e, we can see the temporal loss is most effective for the improvement of temporal consistency.

To further improve the performance, we combine the distillation terms with the temporal loss and achieve the mIoU of 73.06 and temporal consistency of 70.56. We do not increase any parameters or extra computational cost with per-frame inference. Both the distillation terms and the temporal loss can be seen as regularization terms, which can help the training process. Such regularization terms introduce extra knowledge from the pre-trained teacher net and the motion estimation network. Besides, the performance improvement also benefits from the unlabelled data from the video.

Impact of the random sample policy. We apply the random sample (RS) policy when training with video sequence in order to make use of more unlabelled images, and capture the long-term dependency. Experiment results are shown in Table 2. By employing the random sampled policy, both the temporal loss and distillation terms can benefit from the more sufficient training data in the video sequence, and obtain an improvement on mIoU from 0.24% to 0.69% as well as an the temporal consistency from 0.19% to 0.63%. We employ such a random sampled policy considering the memory cost during training. Although employing more frames in the video sequence may improve the performance, it is not friendly to computing resources.

Impact of the teacher net. The temporal loss can improve the temporal consistency of both cumbersome models and compact models. We compare the performance of the student net training with different teacher net (i.e., with and without the proposed temporal loss) to verify that the temporal consistency can be transferred with our designed distillation item. The results are shown in Table 3. The temporal consistency of the teacher net (PSPNet101) can be enhanced by training with temporal loss by 1.97%. Meanwhile, the mIoU can also be improved by 0.69%. By using the enhanced teacher net in the distillation framework, the segmentation accuracy is comparable (70.26 **v.s.** 70.32), but the temporal consistency has a significant improvement (69.27 **v.s.** 70.10), indicating

Table 2 – Impact of the random sample policy. RS: random sample policy, TC: temporal consistency, TL: temporal loss, Dis: distillation items, ALL: combine TL with Dis. The proposed random sample policy can improve the accuracy and temporal consistency.

Method	RS	mIoU	TC
PSPNet18 + TL		70.04	70.21
PSPNet18 + TL	✓	70.67	70.46
PSPNet18 + Dis		71.24	69.48
PSPNet18 + Dis	✓	72.01	69.99
PSPNet18 + ALL		72.87	70.05
PSPNet18 + ALL	✓	73.06	70.56

that the proposed distillation methods can transfer the temporal consistency from the teacher net.

Table 3 – Influence of the teacher net. TL: temporal loss. TC: temporal consistency. We use the pair-wise-frame distillation to show our design can transfer the temporal consistency from the teacher net.

Method	Teacher Model	mIoU	TC
PSPNet101	None	78.84	69.71
PSPNet101 + TL	None	79.53	71.68
PSPNet18	None	69.79	68.50
PSPNet18	PSPNet101	70.26	69.27
PSPNet18	PSPNet101 + TL	**70.32**	**70.10**

4.2 Results

Cityscapes Effectiveness on different compact networks. We apply our training schemes to several efficient semantic segmentation networks: PSPNet18 [40], MobileNetV2 [29] and HRNet-w18 [33, 32]. All the networks are tested with the whole resolution of each frame in the video sequence. The mIoU, temporal consistency, and model parameters are shown in Table 4 and Figure 5. Table 4 shows, the proposed training scheme has a generalization ability for different compact networks and can improve the segmentation accuracy as well as temporal consistency for semantic segmentation models with per-frame inference.
Comparison with state-of-the-art. The compact networks with per-frame inference can be more efficient than keyframe-based or other multi-frame input semantic video segmentation networks. Besides, with per-frame inference, semantic segmentation networks have no unbalanced latency and can handle every frame independently. We follow current state-of-the-art Accel [14] to test all methods on a single GTX 1080Ti GPU, and list the accuracy and the inference

Table 4 – We compare our methods with recent efficient image semantic segmentation networks. TL: temporal loss, Dis: all the distillation items, TC: temporal consistency, #Param: parameters of the networks. Data plotted in Figure 5, and mIou is tested with whole images.

Method	mIoU	TC	#Param
PSPNet18 [40]	69.79	68.50	13.16
PSPNet18 + TL	71.12	69.99	13.16
PSPNet18 + Dis + TL	**73.06**	**70.56**	13.16
MobileNetV2 [29]	70.15	68.38	3.24
MobileNetV2+ TL	70.72	**70.37**	3.24
MobileNetV2+ Dis + TL	**73.92**	69.89	3.24
HRNet-w18 [32, 33]	75.64	69.06	3.92
HRNet-w18 + TL	76.40	69.55	3.92
HRNet-w18 + Dis + TL	**76.60**	**70.14**	3.92

speed in Table 5. Table 5 shows the proposed training schemes can achieve a better trade-off between the accuracy and the inference speed compared with other state-of-the-art semantic video segmentation methods, especially the MobileNetV2 with the fps of 20.8 and mIoU of 73.9.

Qualitative visualization. Qualitative visualization results are shown in Figure 7, in which, we can see, the keyframe-based method Accel-18 will produce unbalanced quality segmentation results between the keyframe (e.g., the orange box of k) and other frames (e.g., the orange box of $k+1$ and $k+3$), due to the different forward-networks it chooses. By contrast, ours can produce stable results on the video sequence because we use the same enhanced network on all frames. Compared with the baseline method trained on single frames, we can see our proposed method can produce more smooth results, e.g., the region in red boxes. Video results can be found in the supplementary material. Moreover, we show a case of the temporal consistency between neighbouring frames in a sampled frame sequence in Figure 6. The temporal consistency between two frames is evaluated by the warping pixel accuracy. The higher the better. The keyframe based method will produce jitters between keyframe and other frames, while our training methods can improve the temporal consistency for every frame. The temporal consistency between other frames are higher than our methods, but the segmentation performance is lower than ours.

CamVid We provide additional experiments on CamVid to show our method is not limited to Cityscapes. We use the MobileNetV2 as the backbone in the PSPNet. In Table 6, the segmentation accuracy, and the temporal consistency are improved compared with the baseline method. We also outperform current state-of-the-art semantic video segmentation methods with a better trade-off between the accuracy and the inference speed. The results are shown in Table 7. We use the pre-trained weight from cityscapes following VideoGCRF [3]. VideoGCRF [3] can achieve 22 fps with 321×321 resolution on a GTX 1080 card, which is reported in their paper. We can achieve 78 fps with the same resolution, which

is faster. The consistent improvements on both datasets show the generalization ability of our training schemes for real-time semantic video segmentation.

5 Conclusions

We propose to use compact networks for efficient semantic video segmentation with a per-frame inference manner. We explicitly consider the temporal correlation during training by using: the temporal loss and the new temporal consistency knowledge distillation. During inferring, the model handles each frame separately, which eases the latency and enables the parallel processing. The compact networks achieve better temporal consistency and semantic accuracy, with no annotation cost and no extra computational cost during inferring. Building upon the efficient MobileNetV2, our method outperform other semantic video segmentation methods with a better trade-off between accuracy and speed. Besides, we verify the effectiveness of all the proposed training schemes, therefore one can choose a part of them or combine them all together in practice according to their needs.

Appendix

A Details of distillation mechanism

A.1 Single frame distillation

Following Liu et.al. [21], we employ pixel-wise distillation and pair-wise distillation for each single frame. For the pixel-wise distillation, we use the class probabilities Q produced from the cumbersome model as soft targets for training the compact network.

The loss function based on the Kullback-Leibler divergence is given as follows,

$$\ell_{pi} = \frac{1}{N}\sum_{i=1}^{N} \mathrm{KL}(\mathbf{q}_i^s \| \mathbf{q}_i^t), \tag{4}$$

where $\mathbf{q}_i$ represent the class probabilities of the ith pixel of the segmentation map and N is the number of the pixels.

The pair-wise distillation is built on the self-similarity map $\mathbf{A}$ as described in multi-frame dependency. We adopt the squared difference to formulate the pair-wise similarity distillation loss,

$$\ell_{pa} = \frac{1}{N^2}\sum_{i=1}^{N}\sum_{i=j}^{N}(a_{ij}^s - a_{ij}^t)^2. \tag{5}$$

The similarity between two pixels is simply computed from the features $\mathbf{f}_i$ and $\mathbf{f}_j$ as $a_{ij} = \mathbf{f}_i^\top \mathbf{f}_j / (\|\mathbf{f}_i\|_2 \|\mathbf{f}_j\|_2)$. The final loss for sing frame distillation is $\ell_{SF}^t = \ell_{pi} + \ell_{pa}$

A.2 Multi-frame distillation

We employ a ConvLSTM [31] unit to capture the correlations among all frames in a video sequence. The input sequence is consists of the self-similarity maps of the feature map for each frame, $\mathcal{A} = \{\dots \mathbf{A}_{\mathbf{F}_{t-1},\mathbf{F}_{t-1}}, \mathbf{A}_{\mathbf{F}_t,\mathbf{F}_t}, \mathbf{A}_{\mathbf{F}_t+1,\mathbf{F}_t+1} \dots\}$. For each time step,the key equations are shown in below:

$$\begin{aligned}
\mathbf{i}_t =& \sigma(\mathbf{W}_{ai} * \mathbf{A}_{\mathbf{F}_t,\mathbf{F}_t} + \mathbf{W}_{hi} * \mathbf{H}_{t-1} + \mathbf{W}_{ei} \circ \mathbf{E}_{t-1} + \mathbf{b}_i) \\
\mathbf{f}_t =& \sigma(\mathbf{W}_{af} * \mathbf{A}_{\mathbf{F}_t,\mathbf{F}_t} + \mathbf{W}_{hf} * \mathbf{H}_{t-1} + \mathbf{W}_{ef} \circ \mathbf{E}_{t-1} + \mathbf{b}_f) \\
\mathbf{E}_t =& \mathbf{f}_t \circ \mathbf{E}_{t-1} + \mathbf{i}_t \circ \tanh(\mathbf{W}_{ae} * \mathbf{A}_{\mathbf{F}_t,\mathbf{F}_t} + \mathbf{W}_{he} * \mathbf{H}_{t-1} + \mathbf{b}_e) \\
\mathbf{o}_t =& \sigma(\mathbf{W}_{ao} * \mathbf{A}_{\mathbf{F}_t,\mathbf{F}_t} + \mathbf{W}_{ho} * \mathbf{H}_{t-1} + \mathbf{W}_{eo} \circ \mathbf{E}_t + \mathbf{b}_o) \\
\mathbf{H}_t =& \mathbf{o}_t \circ \tanh(\mathbf{E}_t)
\end{aligned} \tag{6}$$

where '$\circ$' denotes the Hadamard product,'$*$' denotes the convolution operator, 'σ' is the sigmoid activation function and the activation of input gate i_t controls whether the new input of this time step will be engaged in the memory cell. $\mathbf{f}_t$ controls how much to keep from the past cell status $\mathbf{E}_{t-1}$. o_t decides the propagation from $\mathbf{E}_t$ to the hidden state $\mathbf{H}_t$. $\mathbf{W}$ and $\mathbf{b}$ represent the trainable parameters in the ConvLSTM unit. We employ the memory state of the final time step $\mathbf{E}_T$ as the distillation item, which contains multi-frame dependency. We align the multi-frame dependency from the teacher net and the student net to enhance the performance of the student net. According to [31], the state of ConvLSTM unit can be viewed as the hidden representations of moving objects, therefore the multi-frame dependency distillation can help to transfer the temporal consistency from teacher net to the student net.

B Temporal consistency

B.1 Details of the evaluation metrics

We follow [16] to measure the temporal stability of a video based on the flow warping error between two frames. Different from [16], we use the mIoU score instead of the mean square error to evaluate the semantic segmentation results

$$E_{warp}(\mathbf{Q}_{t-1}, \mathbf{Q}_t) = \frac{\mathbf{Q}_t \cap \hat{\mathbf{Q}}_{t-1}}{\mathbf{Q}_t \cup \hat{\mathbf{Q}}_{t-1}} \tag{7}$$

where $\mathbf{Q}_t$ represents for the predict segmentation map of frame t and $\hat{\mathbf{Q}}_{t-1}$ represents for the warped segmentation map from frame $t-1$ to frame t. We calculate a statistical average warp IoU on each sequence, and using an average mean on the validation set to evaluate the temporal stability:

$$E_{warp} = \frac{1}{N} \sum_{i=1}^{N} \frac{\mathcal{Q}^i \cap \hat{\mathcal{Q}}^i}{\mathcal{Q}^i \cup \hat{\mathcal{Q}}^i} \tag{8}$$

where $\mathcal{Q} = \{\mathbf{Q}_2, \ldots, \mathbf{Q}_T\}$ and $\hat{\mathcal{Q}} = \{\hat{\mathbf{Q}}_1, \ldots, \hat{\mathbf{Q}}_{T-1}\}$. T is the total frames of the sequence and N is the number of the sequence. On Cityscapes [7], we random sample 100 video sequence from the validation set, which contains 3000 images to evaluate the temporal stability. On Camvid [2], we evaluate the temporal stability of the video sequence 'seq05' from the test set.

B.2 Description of videos and visualization results

We include two videos in the supplementary materials, named 'demo_seq00.mp4' and 'val.mp4', to show the improvement of the temporal consistency. Sampled frames are shown in Figure 8 and Figure 9. From the video, we can see that the proposed method can improve the accuracy and the temporal consistency of the segmentation results. We can also observe that in some situations, both our method and the baseline method will produce inconsistent predictions. Figure 10 shows some segmentation results on CamVid dataset. We can observe that the proposed method outperforms the baseline method in the red region.

Table 5 – Accuracy and inference speed on **Cityscapes**. Inference speed is tested on one GTX 1080Ti. Data plotted in Figure 1(b)

Model	mIoU	Inference speed (fps)
Keyframe based methods		
CC [30]	67.7	16.5
DFF [42]	68.7	9.72
DVSN [36]	70.3	19.8
Accel-18 [14]	72.1	3.59
Refinement on multi-frame predictions		
GRFP [24]	69.4	3.17
Per-frame inference		
PSPNet18-Ours	73.1	9.52
HRNet-w18-Ours	**76.6**	18.9
MobileNetV2-Ours	73.9	**20.8**

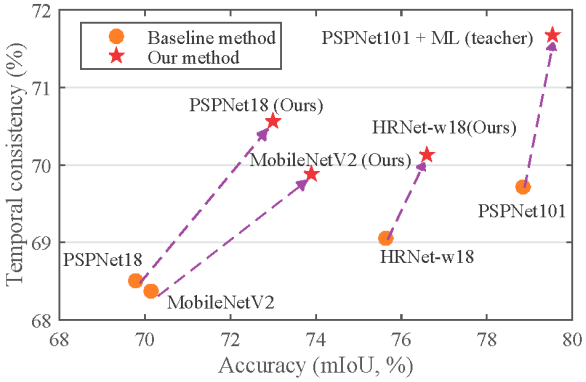

Fig. 5 – **Accuracy vs. temporal consistency.** The improvements for different compact networks. We also show the performance of the enhanced teacher net.

Table 6 – Effectiveness of proposed training schemes on the **CamVid** dataset. TL: temporal loss, Dis: all the distillation items.

Method	mIoU	Temporal consistency
MobileNetV2 [29]	74.39	76.83
MobileNetV2+ TL	76.28	77.59
MobileNetV2+ Dis + TL	**78.19**	**77.86**

Table 7 – Accuracy and inference speed on **CamVid**. We use the MobileNetV2 as the backbone of the PSPNet.

Model	mIoU	Inference speed (fps)
Keyframe based methods		
DFF [42]	66.0	16.1
Accel-18 [14]	66.7	7.14
Refine on multi frames predictions		
GRFP [24]	66.1	6.39
VideoGCRF [3]	75.2	-
Per-frame inference		
MobileNetV2-Ours	78.2	**27.8**

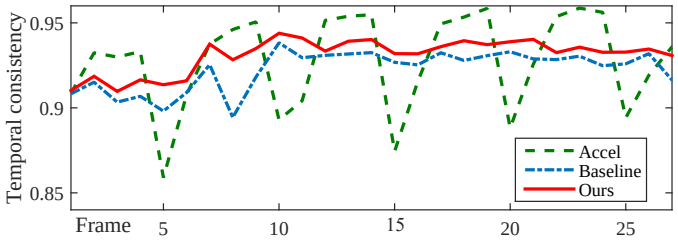

Fig. 6 – The temporal consistency between neighbouring frames in one sampled sequence on Cityscapes. The keyframe based method Accel has severe jitters between keyframes and others.

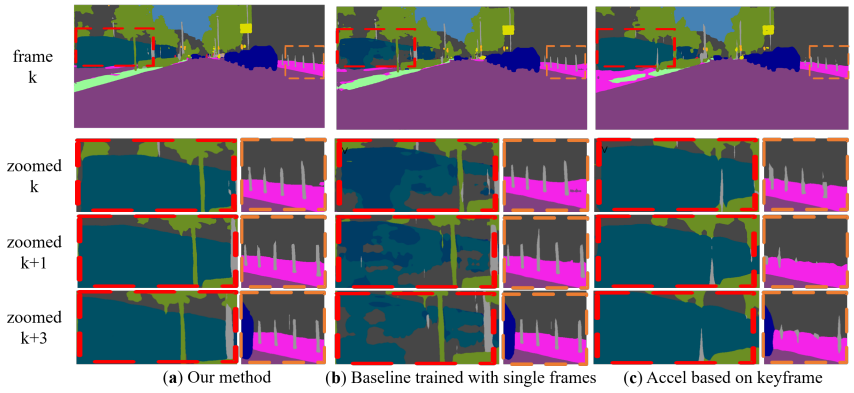

Fig. 7 – **Qualitative outputs.** (**a**): PSPNet18, training on multi frames and inferring on each frame. (**b**): PSPNet18, training and inferring on each frame. (**c**): Accel-18 [14], training and inferring on multi frames. the keyframe is selected in every five frames. For better visualization, we zoom the region in the red and orange box. The proposed method can give more consistent labels to the moving train and the trees in the red box. In the orange boxes, we can see our methods have similar quantity results in each frame while the keyframe based methods may generate worse results in the frame (e.g., $k+3$) which is far from the keyframe (i.e., k).

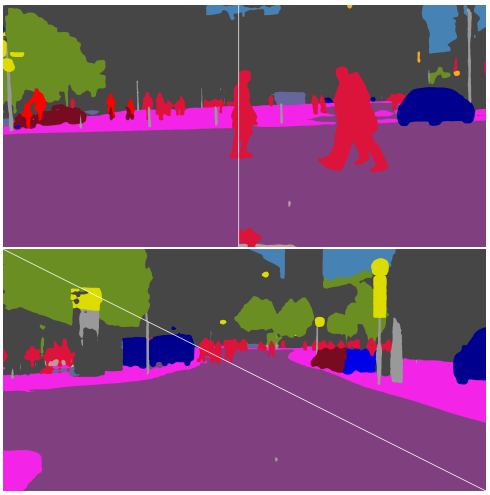

Fig. 8 – Here a white line divides the scene into two parts. 'val.mp4' is the sampled from the validation set we use to evaluate the temporal consistency. In 'val.mp4', our method is shown on the left of the line while the baseline method is on the right. 'demo_seq00.mp4' is the prediction results on the provided demo video 'sequence00' in the Cityscapes dataset, and our method is above the line while the baseline is below the line.

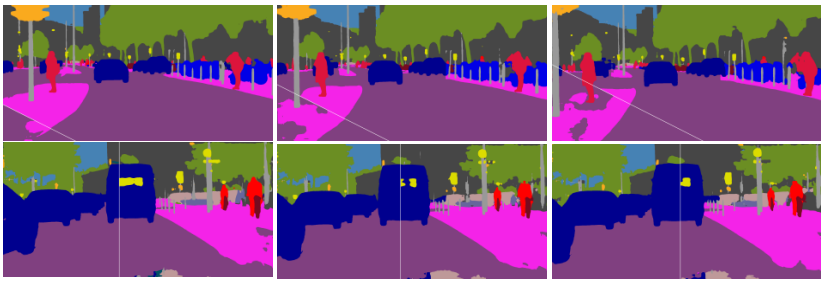

Fig. 9 – Consecutive frames in two videos. **First row**:'demo_seq00.mp4'. Our results are on the top right. **Second row**:'val.mp4'. Our results are on the left. More results can be found in the supplementary videos.

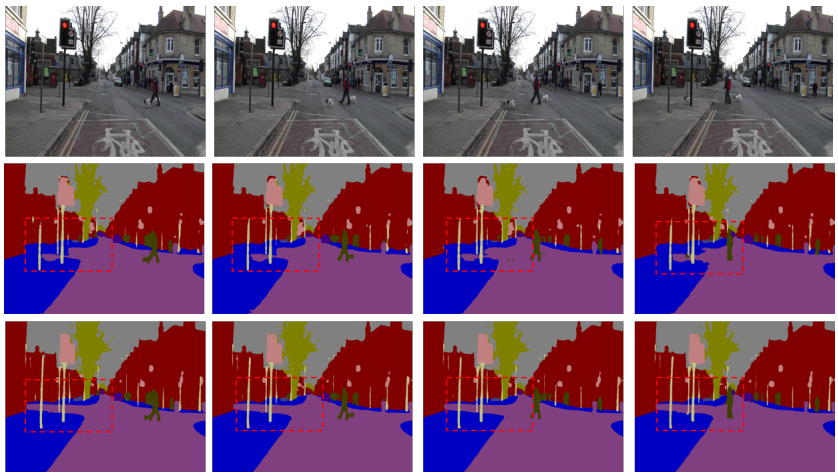

Fig. 10 – Consecutive frames in Camvid dataset. **First row**: input frames. **Second row**: MobileNet trained with cross-entropy loss. **Third row**: MobileNet trained with the temporal loss and distillation items. In the baseline method, the region in the red box keep changing while the proposed method can produce similar results on the still stuff.

References

1. Badrinarayanan, V., Kendall, A., Cipolla, R.: Segnet: A deep convolutional encoder-decoder architecture for image segmentation. IEEE Trans. Pattern Anal. Mach. Intell. (12), 2481–2495 (2017)
2. Brostow, G.J., Shotton, J., Fauqueur, J., Cipolla, R.: Segmentation and recognition using structure from motion point clouds. In: Proc. Eur. Conf. Comp. Vis. pp. 44–57. Springer (2008)
3. Chandra, S., Couprie, C., Kokkinos, I.: Deep spatio-temporal random fields for efficient video segmentation. In: Proc. IEEE Conf. Comp. Vis. Patt. Recogn. pp. 8915–8924 (2018)
4. Chen, L.C., Papandreou, G., Kokkinos, I., Murphy, K., Yuille, A.L.: Deeplab: Semantic image segmentation with deep convolutional nets, atrous convolution, and fully connected crfs. IEEE Trans. Pattern Anal. Mach. Intell. **40**(4), 834–848 (2018)
5. Chen, Y., Wang, N., Zhang, Z.: Darkrank: Accelerating deep metric learning via cross sample similarities transfer. Proc. Eur. Conf. Comp. Vis. (2018)
6. Cheng, J., Tsai, Y.H., Wang, S., Yang, M.H.: Segflow: Joint learning for video object segmentation and optical flow. In: Proc. IEEE Int. Conf. Comp. Vis. pp. 686–695 (2017)
7. Cordts, M., Omran, M., Ramos, S., Rehfeld, T., Enzweiler, M., Benenson, R., Franke, U., Roth, S., Schiele, B.: The cityscapes dataset for semantic urban scene understanding. In: Proc. IEEE Conf. Comp. Vis. Patt. Recogn. (2016)
8. Fayyaz, M., Saffar, M.H., Sabokrou, M., Fathy, M., Huang, F., Klette, R.: Stfcn: spatio-temporal fully convolutional neural network for semantic segmentation of street scenes. In: Proc. Asian Conf. Comp. Vis. pp. 493–509. Springer (2016)
9. Gadde, R., Jampani, V., Gehler, P.V.: Semantic video cnns through representation warping. In: Proc. IEEE Int. Conf. Comp. Vis. pp. 4453–4462 (2017)
10. Gupta, A., Johnson, J., Alahi, A., Fei-Fei, L.: Characterizing and improving stability in neural style transfer. In: Proc. IEEE Int. Conf. Comp. Vis. pp. 4067–4076 (2017)
11. He, K., Zhang, X., Ren, S., Sun, J.: Deep residual learning for image recognition. Proc. IEEE Conf. Comp. Vis. Patt. Recogn. pp. 770–778 (2016)
12. He, T., Shen, C., Tian, Z., Gong, D., Sun, C., Yan, Y.: Knowledge adaptation for efficient semantic segmentation. In: Proc. IEEE Conf. Comp. Vis. Patt. Recogn. pp. 578–587 (2019)
13. Hinton, G.E., Vinyals, O., Dean, J.: Distilling the knowledge in a neural network. arXiv: Comp. Res. Repository **abs/1503.02531** (2015)
14. Jain, S., Wang, X., Gonzalez, J.E.: Accel: A corrective fusion network for efficient semantic segmentation on video. In: Proc. IEEE Conf. Comp. Vis. Patt. Recogn. pp. 8866–8875 (2019)
15. Kim, D., Woo, S., Lee, J.Y., Kweon, I.S.: Deep video inpainting. In: Proc. IEEE Conf. Comp. Vis. Patt. Recogn. pp. 5792–5801 (2019)
16. Lai, W.S., Huang, J.B., Wang, O., Shechtman, E., Yumer, E., Yang, M.H.: Learning blind video temporal consistency. In: Proc. Eur. Conf. Comp. Vis. pp. 170–185 (2018)
17. Levin, A., Lischinski, D., Weiss, Y.: Colorization using optimization. ACM Trans. Graph. **23**(3), 689–694 (2004)
18. Li, Q., Jin, S., Yan, J.: Mimicking very efficient network for object detection. Proc. IEEE Conf. Comp. Vis. Patt. Recogn. pp. 7341–7349 (2017)

19. Li, Y., Shi, J., Lin, D.: Low-latency video semantic segmentation. In: Proc. IEEE Conf. Comp. Vis. Patt. Recogn. pp. 5997–6005 (2018)
20. Liu, S., Wang, C., Qian, R., Yu, H., Bao, R., Sun, Y.: Surveillance video parsing with single frame supervision. In: Proc. IEEE Conf. Comp. Vis. Patt. Recogn. pp. 413–421 (2017)
21. Liu, Y., Chen, K., Liu, C., Qin, Z., Luo, Z., Wang, J.: Structured knowledge distillation for semantic segmentation. In: Proc. IEEE Conf. Comp. Vis. Patt. Recogn. pp. 2604–2613 (2019)
22. Mehta, S., Rastegari, M., Caspi, A., Shapiro, L., Hajishirzi, H.: Espnet: Efficient spatial pyramid of dilated convolutions for semantic segmentation. Proc. Eur. Conf. Comp. Vis. (2018)
23. Miksik, O., Munoz, D., Bagnell, J.A., Hebert, M.: Efficient temporal consistency for streaming video scene analysis. In: 2013 IEEE International Conference on Robotics and Automation. pp. 133–139. IEEE (2013)
24. Nilsson, D., Sminchisescu, C.: Semantic video segmentation by gated recurrent flow propagation. In: Proceedings of the IEEE Conference on Computer Vision and Pattern Recognition. pp. 6819–6828 (2018)
25. Paszke, A., Chaurasia, A., Kim, S., Culurciello, E.: Enet: A deep neural network architecture for real-time semantic segmentation. arXiv: Comp. Res. Repository **abs/1606.02147** (2016)
26. Reda, F., Pottorff, R., Barker, J., Catanzaro, B.: flownet2-pytorch: Pytorch implementation of flownet 2.0: Evolution of optical flow estimation with deep networks. https://github.com/NVIDIA/flownet2-pytorch (2017)
27. Romera, E., Alvarez, J.M., Bergasa, L.M., Arroyo, R.: Efficient convnet for real-time semantic segmentation. In: IEEE Intelligent Vehicles Symp. pp. 1789–1794 (2017)
28. Romero, A., Ballas, N., Kahou, S.E., Chassang, A., Gatta, C., Bengio, Y.: Fitnets: Hints for thin deep nets. arXiv: Comp. Res. Repository **abs/1412.6550** (2014)
29. Sandler, M., Howard, A., Zhu, M., Zhmoginov, A., Chen, L.C.: Mobilenetv2: Inverted residuals and linear bottlenecks. In: Proc. IEEE Conf. Comp. Vis. Patt. Recogn. (2018)
30. Shelhamer, E., Rakelly, K., Hoffman, J., Darrell, T.: Clockwork convnets for video semantic segmentation. In: Proc. Eur. Conf. Comp. Vis. pp. 852–868. Springer (2016)
31. SHI, X., Chen, Z., Wang, H., Yeung, D.Y., Wong, W.k., WOO, W.c.: Convolutional lstm network: A machine learning approach for precipitation nowcasting. In: Proc. Advances in Neural Inf. Process. Syst. pp. 802–810 (2015)
32. Sun, K., Xiao, B., Liu, D., Wang, J.: Deep high-resolution representation learning for human pose estimation. In: Proc. IEEE Conf. Comp. Vis. Patt. Recogn. (2019)
33. Sun, K., Zhao, Y., Jiang, B., Cheng, T., Xiao, B., Liu, D., Mu, Y., Wang, X., Liu, W., Wang, J.: High-resolution representations for labeling pixels and regions. arXiv: Comp. Res. Repository **abs/1904.04514** (2019)
34. Tian, Z., He, T., Shen, C., Yan, Y.: Decoders matter for semantic segmentation: Data-dependent decoding enables flexible feature aggregation. In: Proc. IEEE Conf. Comp. Vis. Patt. Recogn. pp. 3126–3135 (2019)
35. Tsai, Y.H., Yang, M.H., Black, M.J.: Video segmentation via object flow. In: Proc. IEEE Conf. Comp. Vis. Patt. Recogn. pp. 3899–3908 (2016)
36. Xu, Y.S., Fu, T.J., Yang, H.K., Lee, C.Y.: Dynamic video segmentation network. In: Proc. IEEE Conf. Comp. Vis. Patt. Recogn. pp. 6556–6565 (2018)
37. Yao, C.H., Chang, C.Y., Chien, S.Y.: Occlusion-aware video temporal consistency. In: Proc. ACM Int. Conf. Multimedia. pp. 777–785. ACM (2017)

38. Zagoruyko, S., Komodakis, N.: Paying more attention to attention: Improving the performance of convolutional neural networks via attention transfer. Proc. Int. Conf. Learn. Representations (2017)
39. Zhao, H.: Semseg. https://github.com/hszhao/semseg (2019)
40. Zhao, H., Shi, J., Qi, X., Wang, X., Jia, J.: Pyramid scene parsing network. In: Proc. IEEE Conf. Comp. Vis. Patt. Recogn. pp. 2881–2890 (2017)
41. Zhu, X., Dai, J., Yuan, L., Wei, Y.: Towards high performance video object detection. In: Proc. IEEE Conf. Comp. Vis. Patt. Recogn. pp. 7210–7218 (2018)
42. Zhu, X., Xiong, Y., Dai, J., Yuan, L., Wei, Y.: Deep feature flow for video recognition. In: Proc. IEEE Conf. Comp. Vis. Patt. Recogn. pp. 2349–2358 (2017)
43. Zhu, Y., Sapra, K., Reda, F.A., Shih, K.J., Newsam, S., Tao, A., Catanzaro, B.: Improving semantic segmentation via video propagation and label relaxation. In: Proc. IEEE Conf. Comp. Vis. Patt. Recogn. pp. 8856–8865 (2019)